Synthesis, Characterization, and Evaluation of MCF-7 (Breast Cancer) for Schiff, Mannich Bases, and Their Complexes

Ali Mudher Abdulkareem Al-Khazraji*

Department of Chemistry, College of Education for Pure Science Ibn Al-Haitham, University of Baghdad, Baghdad 10011, Iraq

* ***Corresponding author:***

tel: +964-7724031983
email: ali.m.ak@ihcoedu.uobaghdad.edu.iq

Received: July 18, 2023
Accepted: August 28, 2023

DOI: 10.22146/ijc.87003

Abstract: *A new synthesis of Schiff (K) 6 and Mannich bases (Q) 7 had formed compound (Q) 7 by reacting compound (K) with* N*-methylaniline at the presence of formalin 35% to given Mannich base (Q). Additionally, new complexes were formed by reacting Schiff base (K) with metal salts* $CuCl_2 \cdot 2H_2O$, $PdCl_2 \cdot 2H_2O$, *and* $PtCl_6 \cdot 6H_2O$ *by 2:1 of M:L ratio. New ligands and their complexes were characterized, exanimated, and confirmed through several techniques, including FTIR, UV-visible,* ^{1}*H-NMR,* ^{13}*C-NMR spectroscopy, CHN analysis, FAA, TG, molar conductivity, and magnetic susceptibility. These compounds and their complexes were screened against breast cancer cells. It was determined that several of these compounds had a significant anti-breast cancer effect due to their ability to induce cell death and reduce tumor growth. Metal complexes have been thoroughly studied as a potential anti-cancer therapy and have shown promising results. It was revealed these complexes uniquely affect the biological processes involved in cancer growth, leading to apoptosis and fading of cells. To form MCF-7 cell cultures, MCF-7 cells were seeded in 96-well plates at an appropriate density (*5×10^5 *cells/well). Metal complexes utilized in MCF-7 therapy have the potential to disband some of the harms associated with chemotherapy, such as drug resistance and toxicity.*

Keywords: *Schiff base; Mannich base; breast cancer; apoptosis; MCF-7 cells*

■ INTRODUCTION

Schiff base is a functional group consisting of an imine (-C=N-) or azomethine (-N=CH-) linkage, which is formed by the condensation of a primary amine with an aldehyde or ketone [1-2]. It is named after its discoverer, Hugo Schiff, who synthesized it in 1864. Schiff bases have numerous applications in various fields, including chemistry, biology, and medicine. They have been used as ligands for metal ions in catalysis and as intermediates in synthesizing various organic compounds. Schiff bases also have important biological activities, including antimicrobial, antitumor, and antiviral properties. Evidence suggests that 1,2,4-triazole derivative Schiff bases exhibit anti-cancer activity against MCF-7 cells [3-4]. For instance, past research investigated the anti-cancer activity of a series of Schiff bases derived from 1,2,4-triazole and found that some of the tested compounds showed potent cytotoxicity against MCF-7 cells [5]. Other research evaluated the cytotoxicity of a series of 1,2,4-triazole Schiff bases and their corresponding platinum(VI) complexes against MCF-7 cells and found that some of the tested compounds showed promising anti-cancer activity. Some studies also reported the cytotoxicity of Schiff bases derived from 1,2,4-triazole against breast cancer, suggesting that their potential as anti-cancer agents against breast cancer cells.

Mannich bases are organic compounds that contain an amine, a carbonyl group, and an aromatic ring [6]. They are used in a variety of applications, including as antimicrobial agents and as inhibitors of enzymes involved in cancer cell growth. Mannich bases have been studied for their potential to inhibit the growth of breast cancer cells. Studies have shown that the effects of Mannich based on the growth of MCF-7 cells were found to inhibit cell growth in a dose-dependent manner. Other research reported that

Mannich bases could induce apoptosis in MCF-7 cells [7]. Another study investigated the effects of Mannich bases on the expression of genes involved in the growth and survival of MCF-7 cells. The results demonstrated that Mannich bases could downregulate the expression of genes involved in cell growth and survival, suggesting that they may effectively inhibit the growth of MCF-7 cells. Overall, evidence to date suggests that Mannich bases may effectively inhibit the growth of MCF-7 cells.

Several empirical studies have demonstrated the potential of heterocyclic compounds to target breast cancer, advocating the potential of heterocyclic compounds to show anti-breast cancer activity. Both heterocyclic steroids and curcumin were found to have a significant effect on the viability of MCF-7 cells when treated for 48 h. Heterocyclic drug aripiprazole also demonstrated a growth inhibitory potential against cancer cells and could serve as a lead for developing novel breast cancer drugs. Furthermore, platinum(IV) complexes were reported to be a highly potent antiproliferative activity against all the tested cancer cell lines, including the well-known refractory triple-negative breast cancer cell line MCF-7. Besides, etoposide was found to inhibit the proliferation, migration, and invasion of MCF-7 cells [8]. Furthermore, the biotin-guided platinum(IV) complex is highly cytotoxic against cancer cells but hypo-toxic against mammary epithelial cells [9]. MCF-7 is a commonly used breast cancer cell line that is highly responsive to chemotherapy [10]. Schiff and Mannich base ligands were synthesized, and used to form metal complexes with copper, palladium, and platinum ions. Spectroscopic techniques and other analyses were employed to identify the ligands and complexes. The complexes exhibited octahedral structures, except for palladium, which had a tetrahedral geometry.

This paper presents results from *in vitro* experiments examining the effects of synthetic compounds derived from ligands on breast cancer progression. The study focused on the MCF-7 cell line and used the MTT assay to assess cell proliferation. The findings suggest that certain synthetic compounds, even at low concentrations, have the ability to inhibit the growth of breast cancer cells. The effectiveness of these compounds was ranked as follows: Pt_2K > Q > Pd_2K > Cu_2K > K > untreated cells. These findings have important implications for the potential development of new treatments for breast cancer.

■ EXPERIMENTAL SECTION

Materials

The Sigma-Aldrich company supplied all the chemicals utilized in this research with additional purification. These chemicals and solvents included terephthalic acid, pure ethanol (EtOH), carbon-disulfide (CS_2), chemical compounds (glacial acetic acid, sulfuric acid, and potassium hydroxide (KOH)), sodium bicarbonate ($NaHCO_3$), diethyl ether, metal salt ($CuCI_2{\cdot}2H_2O$, $PdCI_2{\cdot}2H_2O$, and $PtCI_6{\cdot}6H_2O$), trypsin/EDTA, DMSO-d_6, Roswell Park Memorial Institute (RPMI) 1640, 3-(4,5-dimethylthiazol-2-yl)-2,5-diphenyltetrazolium bromide (MTT) stain, and fetal bovine serum (FBS).

Instrumentation

This study adopted the KBr-disk technique to record the Fourier transform infrared (FTIR) spectra on a Shimadzu-8400 spectrophotometer (Shimadzu, Kyoto, Japan). A Bruker DRX400 NMR spectrometer (Bruker, Zürich, Switzerland) was used to record the proton nuclear spectra for Schiff base (K) magnetic resonance (^{1}H-NMR, ^{13}C-NMR) spectra (400 MHz, 125 MHz) in DMSO-d_6 related to tetramethylsilane. Conductivity measurements were conducted with the WTW, (USA). The chloride content was 686–Titro Processor–665 Dosim A–Metrohm/Swiss. The magnetic susceptibility measurements were done using the Bruker-BM6 instrument, while the electronic spectra used a Shimadzu-160 spectrophotometer (200–900 nm; Kyoto, Japan). The atomic absorption (AA) technique was conducted using a Shimadzu PR-5 ORAPHIC-PRINTER atomic absorption spectrophotometer, while the Gallen Kamp apparatus determined the melting point. Additionally, the Vario-EL III elemental instrument was applied to conduct the elemental analysis. This study also used the CO_2 incubator Cypress Diagnostics (Belgium), Microtiter reader Gennex lab

(USA), Laminar flow hood K & K scientific supplier (Korea), microscope TE-2000 (Nikon, Japan), and cell culture plates Santa Cruz Biotechnology (USA).

Procedure

Synthesis of ethyl (E)-3-(4-hydroxyphenyl)acrylate (2)

The routing Scheme 1 was utilized to produce ethyl (*E*)-3-(4-hydroxyphenyl)acrylate [11]. It was synthesized in 5 g (0.027 mmol) of (*E*)-3-(4-hydroxyphenyl)acrylic acid (1), dissolved in 40 mL EtOH, and utilized dropwise through 6 mL of conc. H_2SO_4 was the media phase of the acidic solution. The mixture of reaction was placed under reflux for 6 h, and the residual acid was eliminated by vacuum filtering. A $NaHCO_3$ solution 10%, 50 mL was used to produce the ethyl (*E*)-3-(4-hydroxyphenyl)acrylate (2) compound, followed by an assembly of the crystal.

Synthesis of (E)-3-(4-hydroxyphenyl)acrylohydrazide (3)

This route was utilized to synthesize (*E*)-3-(4-hydroxyphenyl) acrylic hydrazide Scheme 1 [12]: 3.3 g (0.017 mmol) of ethyl (*E*)-3-(4-hydroxyphenyl)acrylate was immersed in 25 mL of absolute EtOH. The mixture of solution was heated and refluxed for 8 h before hydrazine hydrate 80% 35 mL was added, and the reaction was assessed using TLC. Eventually, vacuum-dried and filtered solids were produced via a Paige crystal needle with ice-cold water in the form of powder.

Synthesis of potassium (E)-2-(3-(4-hydroxyphenyl) acryloyl)hydrazine-1-carbodithioate (4)

In Scheme 1, an EtOH solution was utilized to dissolve each of the compounds: 2 g (0.006 mmol) of (*E*)-3-(4-hydroxyphenyl)acrylohydrazide (3) and 1 g (0.0135 mmol) of KOH, resulting in the formation of compound potassium (*E*)-2-(3-(4-hydroxyphenyl)acryloyl)hydrazine-1-carbodithioate (4). Then, CS_2 was added to the mixture solution at 0 °C for 12 h. To precipitate the compound, diethyl ether (250 mL) was added, and the mixture was refluxed with continuous stirring. It was later cooled for 10 min, and the resulting solid crystal was obtained by vacuum filtration.

Synthesis of (E)-4-amino-5-(4-hydroxystyryl)-2,4-dihydro-3H-1,2,4-triazole-3-thione (5)

The current procedure in Scheme 1 was utilized to synthesize compound 5, (*E*)-4-amino-5-(4-hydroxystyryl)-2,4-dihydro-3*H*-1,2,4-triazole-3-thione, from compound 4, (*E*)-2-(3-(4-hydroxyphenyl)acryloyl) hydrazine-1-carbodithioate (2.86 g, 0.0098 mmol), and 80% hydrazine hydrate (30 mL). The mixture was allowed to react for 6 h, resulting in a greenish solution. TLC analysis was performed to monitor the reaction's progress. The solution became acidic under vacuum, and the resulting precipitate was collected.

Synthesis of compound 4,4'-(((1Z,1'Z)-1,4-phenylenebis(methaneylylidene))bis(azaneylylidene))bis(5-((E)-4-hydroxystyryl)-2,4-dihydro-3H-1,2,4-triazole-3-thione) (K) (6)

A hot solution of (*E*)-4-amino-5-(4-hydroxystyryl)-2,4-dihydro-3*H*-1,2,4-triazole-3-thione (1.41 g, 0.0025 mmol) in 30 mL of EtOH was added dropwise to a solution of terephthaldehyde (1.34 g, 0.01 mmol) in the presence of 6 drops of glacial acetic acid (AcOH). The reaction mixture was refluxed for 8 h. The resulting white compound was filtered and dried in air to yield the required Schiff base ligand (K) as a white solid crystal (yield: 72%, m.p.: 291 °C) in Scheme 1.

General synthesis of 4,4'-(((1Z,1'Z)-1,4-phenylenebis (methaneylylidene))bis(azaneylylidene))bis(5-((E)-4-hydroxystyryl)-2-((methyl(phenyl)amino)methyl)-2,4-dihydro-3H-1,2,4-tr iazole-3-thione) (Q) (Mannich base) (7)

In Scheme 1: 0.84 g of Schiff base (K) 6 (0.0015 mmol) and 35% methylene oxide (0.3 g, 2 mmol) were dissolved in ethanol (12 mL), and the mixture was stirred at room temperature for 20 min. A solution of *N*-methylaniline (0.5 g, 0.9 mmol) in EtOH (4 mL) was slowly added dropwise. The reaction mixture was stirred for 3–4 h and placed in a refrigerator overnight. The resulting precipitate was filtered and recrystallized from ethanol to give Mannich base 7.

Synthesis of the transition metal complexes (8)

The complexes (Cu_2K, Pd_2K and Pt_2K) were synthesized as shown in Scheme 1 by adding the hot ethanolic solution of the metal ions ($CuCl_2{\cdot}2H_2O$, $PdCl_2{\cdot}2H_2O$, and $PtCl_6{\cdot}6H_2O$) to 0.93 g (0.0016 mmol) of hot ligand (K) in 2:1 (metal:ligand) molar ratio. The reaction mixture was refluxed for 8 h, and colored precipitates were formed. The complexes obtained were

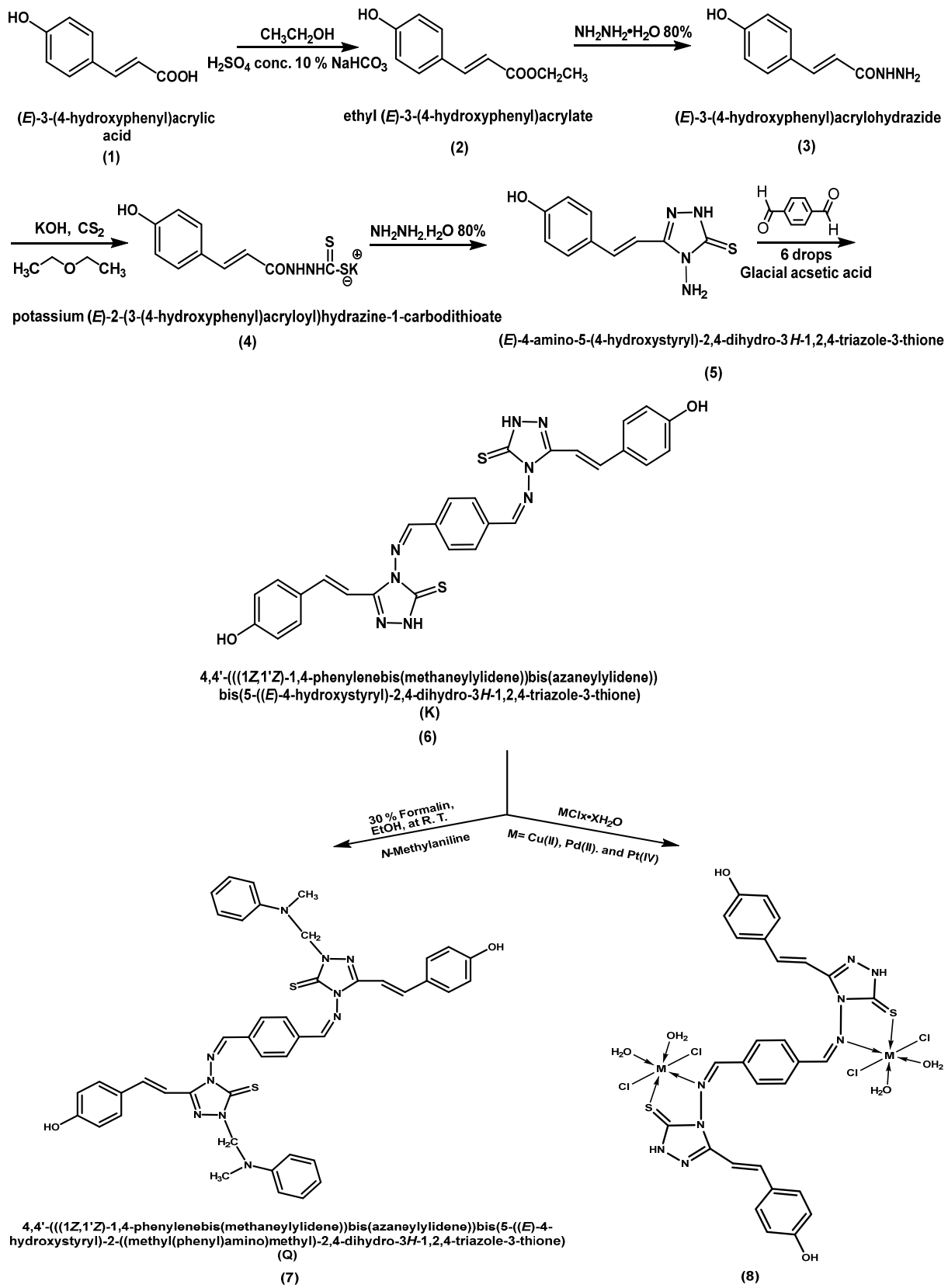

Scheme 1. A common synthesis pathway for new Schiff, Mannich bases, and their complexes

filtered and recrystallized from EtOH. Table 1 shows the number of metal salts in the complexes.

Cell toxicity tests (MTT assay) and staining combining ethidium bromide with acridine orange (AO/EB) for MCF-7 cells

To maintain the cell cultures of MCF-7, a human breast cancer cell line, the MCF-7 cells were seeded at an appropriate density (5×10^5 cells/well) in 96-well plates and incubated for 72 h to allow the cells to attach and grow in cell culture plates that were previously coated with an appropriate substrate. Media MCF-7 cells can be grown in a variety of media RPMI 1640 medium, supplemented with 10% FBS [13] and antibiotics such as 100 unit/mL penicillin and 100 g/mL streptomycin [14]. Culture conditions cells should be cultured for 180 min at 37 °C in a humidified incubator with 5% CO_2. Once the cells reached approximately 80% confluency, they were detached from the plate by adding trypsin-EDTA solution, incubated for 60 min, neutralized with media, and re-suspended and seeded at the desired density in new plates. Quality control was done to regularly check the health and morphology of the cells under a microscope to ensure that they were growing as expected. It was also important to routinely check for potential contamination by cell lines. Cryopreservation was used to preserve cell lines for long-term storage, in which the MCF-7 cells can be cryopreserved in a freezing medium containing dimethyl sulfoxide (DMSO-d_6) [15]. Overall, maintaining MCF-7 cell cultures required careful diligence and adherence to sterile techniques to ensure the purity and viability of the cells. MCF-7 cells in 96-well plates were treated with new compounds at IC_{50} concentrations, and the cells were monitored using fluorescence microscopy after 24 h of incubation, two rounds of washing with PBS, and an injection of 100 µL of AO/EtBr for 2 min.

■ RESULTS AND DISCUSSION

Table 1 provides data from the C, H, N, and S analyses and the atomic absorption of a newly determined ligand derived from the Schiff and Mannich bases, as well as its physical properties. The ligand and its complexes were formed in a 2:1 ratio (metal ion to ligand). All complexes were confirmed to exhibit solubility in DMSO-d_6.

FTIR, ^{1}H-NMR and ^{13}C-NMR of New Schiff Base (K), Mannich Base (Q), and Their Complexes

Analytical data for FTIR, ^{1}H, ^{13}C-NMR for synthesized Schiff, Mannich bases, and other complexes observed in Table 2, and Fig. 1–5: Schiff base (K); FTIR (KBr, ν, cm^{-1}): 3632 (O–H str.), 3335 (N–H str.), 2573 (S–H str.), 1631 (C=N str.) [16], 1329 (C–N str.), 1236 (C=S str.) and 1109 (C–O str.). ^{1}H-NMR (DMSO-d_6, δ ppm): 12.95 (2H, s, S–H thiol), 10.53 (2H, s, O–H alcohol), 9.92 (2H, s, CH=N imine), 9.28 (4H, s, ArH benzene ring central) 7.92 (4H, s, ArH benzene ring terminal), and 6.39 (4H, m, CH=CH ethylene group). ^{13}C-NMR (DMSO-d_6, δ ppm): 157.2 (C–S thiol), 153.4 (C–O alcohol), 140.5 (C=N imine), 137.4 (C=N triazole ring), 126.6 (C=C benzene ring central), 121.99 (C=C benzene terminal), and 105.5 (C=C ethylene). Mannich base (Q); FTIR (KBr,

Table 1. The physical properties and analytical data of the ligand and its complexes are derived from new Schiff (K) and Mannich bases (Q)

Comp.	Experimental formula	Color	M.P (°C)	Yield (%)	M.wt (g mol^{-1})	Micro elemental analysis found (calc.)				Metal content
						C%	H%	N%	S%	% found. (calc.)
K	$C_{28}H_{22}N_8O_2S_2$	White	291	72	566.66	58.11 (59.35)	3.21 (3.91)	18.21 (19.77)	10.84 (11.32)	-
Q	$C_{44}H_{40}N_{10}O_2S_2$	Pale crystal	279	74	804.99	64.39 (65.65)	4.33 (5.01)	15.89 (17.40)	6.05 (7.97)	-
Cu_2K	$C_{28}H_{32}Cl_4Cu_2N_8O_6S_2$	Brown	> 323	79	909.63	35.33 (36.97)	3.09 (3.55)	12.04 (12.32)	6.53 (7.05)	12.76 (13.97)
Pd_2K	$C_{28}H_{32}Cl_4N_8O_6Pd_2S_2$	Pale green	> 317	81	995.37	33.24 (33.79)	2.83 (3.24)	10.21 (11.26)	4.93 (6.44)	20.44 (21.38)
Pt_2K	$C_{28}H_{24}Cl_8N_8O_2Pt_2S_2$	Dark brown	> 311	77	1242.44	25.79 (27.07)	1.57 (1.95)	8.53 (9.02)	4.59 (5.16)	30.22 (31.40)

Table 2. FTIR data for new Schiff (K), Mannich (Q), and metal ion complexes

Symbol	FTIR (ν, cm^{-1})							
	N–H	C=N	C=S	-N–CH_2–N-	M–N	M–O	M–S	M–CI
K	3335	1631	1236	-	-	-	-	-
Q	3311	1612	1225	1166	-	-	-	-
Cu_2Q	3382	1702	1184	-	622	510	466	375
Pd_2Q	3338	1694	1195	-	582	533	452	382
Pt_2Q	3364	1687	1242	-	601	541	432	359

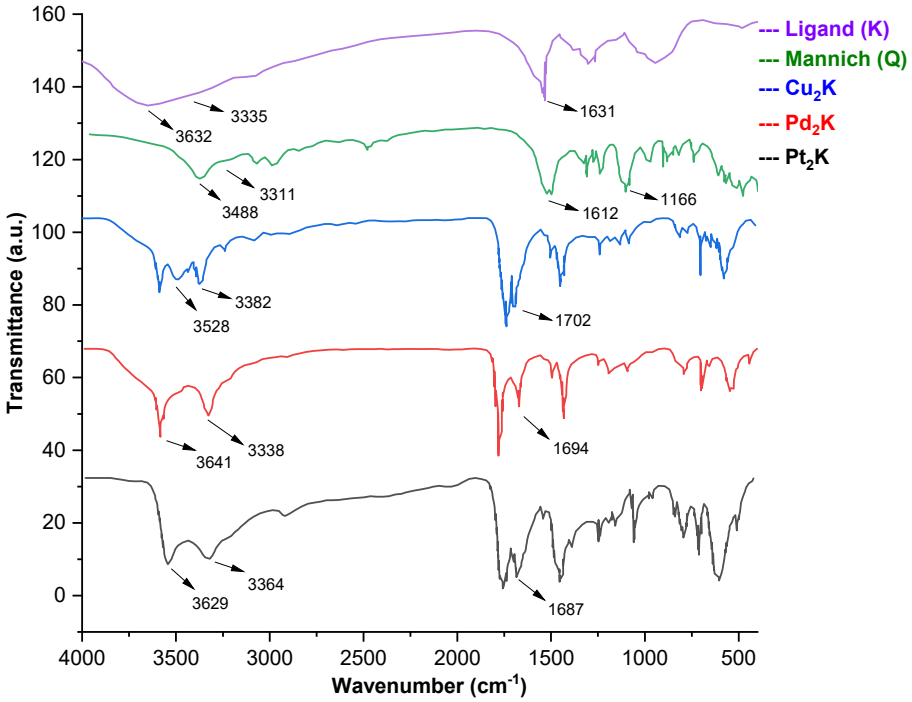

Fig 1. FTIR spectra of Schiff (K), Mannich (Q), and their metal ion complexes

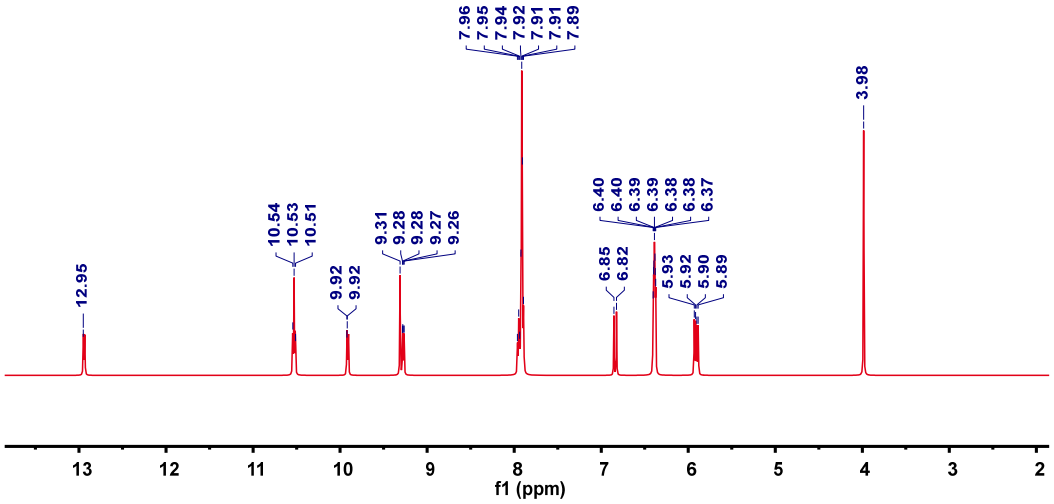

Fig 2. ^{1}H-NMR spectrum of Schiff base (ligand K)

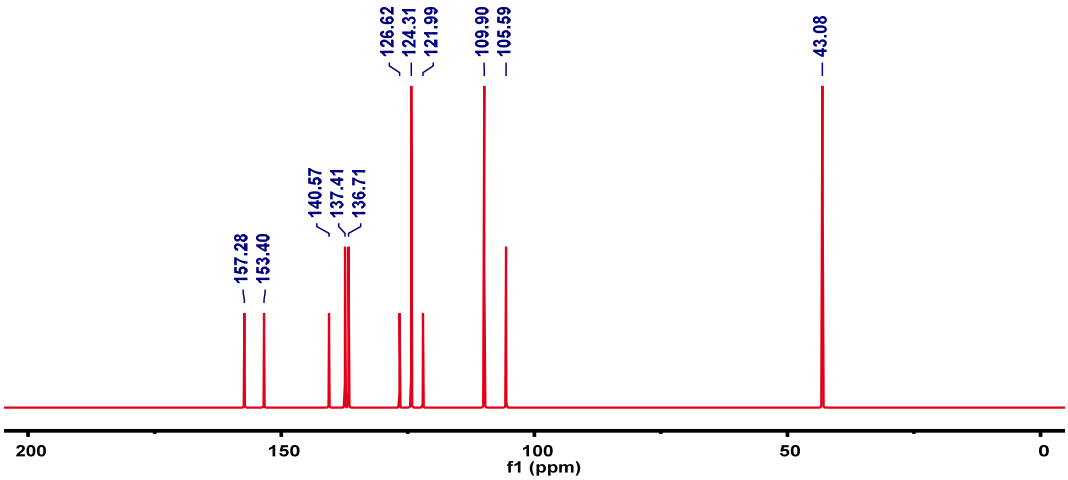

Fig 3. ^{13}C-NMR spectrum of Schiff base (ligand K)

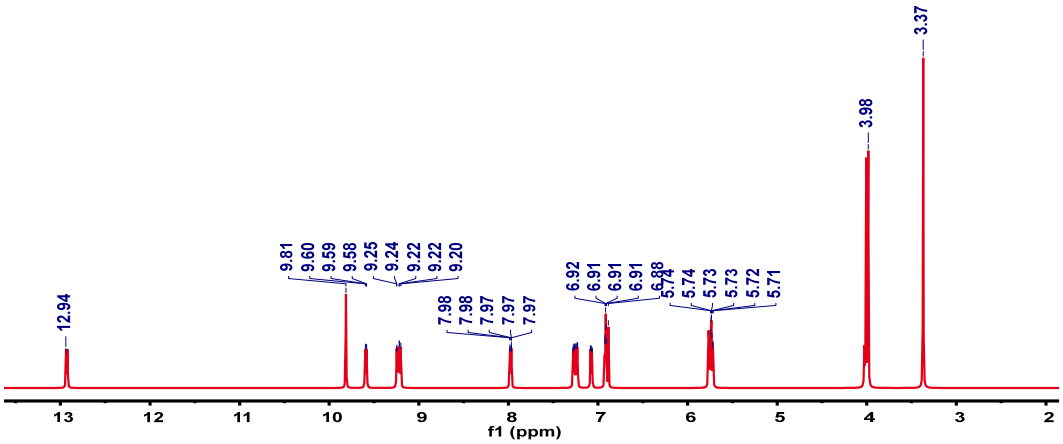

Fig 4. ^{1}H-NMR spectrum of Mannich base (Q)

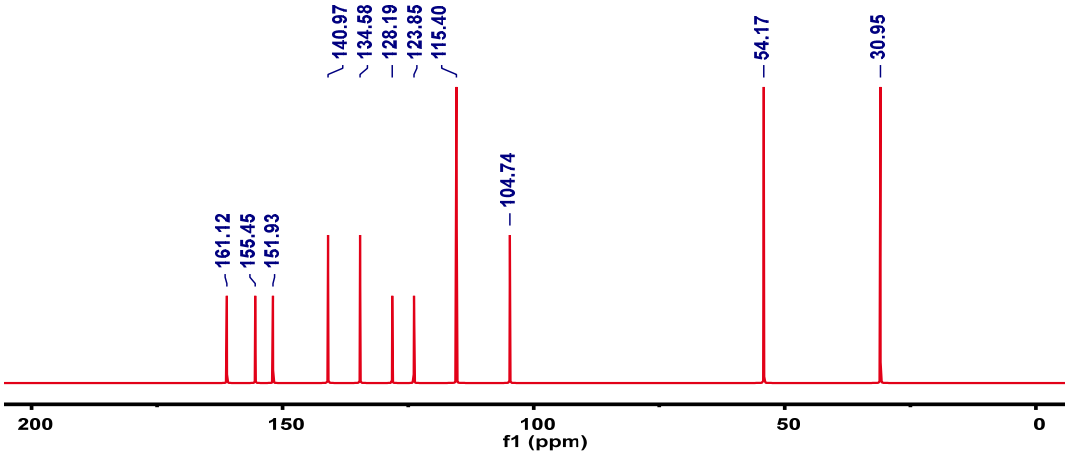

Fig 5. ^{13}C-NMR spectrum of Mannich base (Q)

ν, cm^{-1}): 3488 (O–H str.), 3311 (N–H str.), 2562 (S–H str.), 1612 (C=N str.), 1305 (C–N str.), 1225 (C=S str.), 1124 (C–O str.), and 1166 (-N–CH_2–N- str. Mannich). ^{1}H-NMR (DMSO-d_6, δ ppm): 12.94 (2H, s, S–H thiol),

9.81 (2H, s, O–H alcohol), 9.25 (2H, s, CH=N imine), 7.98 (4H, s, ArH benzene ring central) 7.23 (4H, s, ArH benzene ring terminal), and 6.88 (4H, m, CH=CH ethylene group), 3.37 (4H, s, methylene group Mannich) [17]. ^{13}C-NMR (DMSO-d_6, δ ppm): 161.1 (C-S thiol), 155.4 (C–O alcohol), 151.9 (C=N imine), 140.9 (C–N *N*-methylaniline), 134.5 (C=N triazole ring), 128.1 (C=C ethylene group), 54.1 (CH_2– ethyl group Mannich), 30.9 (CH_3–N Mannich). The FTIR for other complexes (CsI, ν, cm^{-1}) Cu_2K, Pd_2K, and Pt_2K was assigned to M–N, M–O, M–S, and M–Cl, respectively, 622, 510, 466, and 375; 582, 533, 452, and 382; 601, 541, 432, and 359.

The Ultraviolet Spectra of the New Schiff Base (K), Mannich Base (Q), and Their Complexes

The Schiff bases were dissolved in chloroform, and their complexes were formed, resulting in various bands as observed in Table 3 and Fig. 6. The ligand Schiff base (K) exhibited three absorption bands at 365 nm, 27397 cm^{-1}, and 448 nm, 22321 cm^{-1} allocated to π→π*, n→π* intra-ligand transition, and at 560 nm, 17857 cm^{-1} for n→π*. Whereas other complexes were arranged to copper(II) complex at 561 nm, 17825 cm^{-1}, and 739 nm, 13531 cm^{-1} assigned to [^{2}Eg→^{2}T$_2$g] and [L→Cu] (C.T.); palladium(II) complex were assigned to 489 nm, 20449 cm^{-1}, 612 nm, 16339 cm^{-1}, and 723 nm, 13831 cm^{-1} for [^{1}A$_1$g→^{1}B$_1$g], [^{1}A$_1$g→^{1}E$_1$g] and [L→Pd] (C.T.); platinum(IV) complex were assigned to 512 nm, 19531 cm^{-1}, 633 nm, 15797 cm^{-1}, and 709 nm, 14104 cm^{-1} [1A$_1$g→^{3}T$_1$g], [^{1}A$_1$g→^{3}T$_2$g] and [L→Pt] (C.T.). The Mannich base (Q) third bands appearance was assigned to 333 nm, 30030 cm^{-1} and 488 nm, 20491 cm^{-1}, allocated to π→π*, n→π* intra-ligand transition, and 510 nm, 19607 cm^{-1} assigned to n→π*.

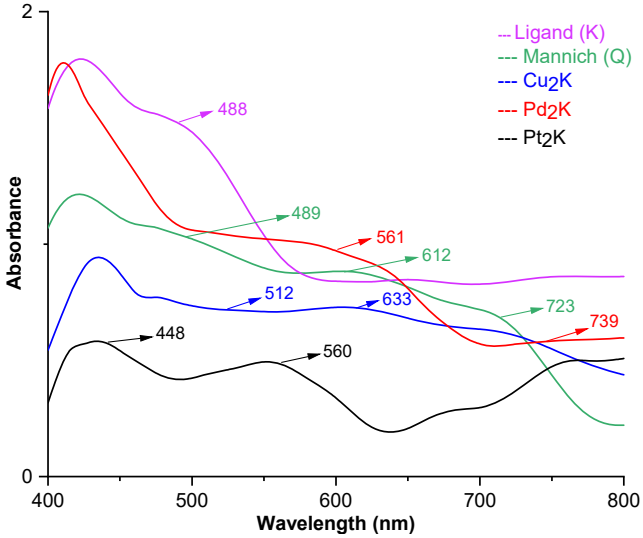

Fig 6. Electronic spectra of the ligand K, Mannich Q, and their metal complexes

Table 3. Molar conductivity, magnetic susceptibility, and electronic spectral data of ligand (K), Mannich (Q), and metal complexes

Compound	$\lambda_{max\ nm}$ (ν cm^{-1})	Assignment	Molar conductivity $Ohm^{-1}\ cm^2\ mol^{-1}$	Magnetic susceptibility (B.M.) (calc.) found	Suggested geometry
Ligand K	365 (27397)	(π→π*)			
	448 (22321)	(n→π*)	-	-	-
	560 (17857)	(n→π*)			
Mannich Q	333 (30030)	(π→π*)			
	488 (20491)	(n→π*)	-	-	-
	510 (19607)	(n→π*)			
Cu_2K	561 (17825)	^{4}Eg→^{4}T$_2$g	13.780	(1.730) 1.900	Octahedral geometry
	739 (13531)	L→Cu C.T.			
Pd_2K	489 (20449)	^{1}A$_1$g→^{1}B$_1$g			
	612 (16339)	^{1}A$_1$g→^{1}E$_1$g	17.210	(0.008) 0.004	Square planar geometry
	723 (13831)	L→Pd C.T.			
Pt_2K	512 (19531)	^{1}A$_1$g→^{3}T$_1$g			
	633 (15797)	^{1}A$_1$g→^{3}T$_2$g	23.410	(0.010) 0.014	Octahedral geometry
	709 (14104)	L→Pt C.T.			

Thermal Analysis (TG) of the New Schiff Base (K), Mannich Base (Q), and Their Respective Complexes

According to Table 4 and Fig. 7, the Schiff and Mannich base ligands (referred to as K and Q) and their complexes underwent TG analysis in the N_2 environment. The analysis was conducted over a 25 to 600 °C temperature range with a heating rate of 10 °C/min. TG analysis is a sensitive method that can assess how changes in physical and chemical properties (e.g., heat capacity) are related to temperature by combining moisture in the oven with gravimetric analysis. The weight loss in the analysis occurred primarily during the later stages of disintegration, resulting in an overall weight loss [18] exceeding 70%. This weight loss was attributed to the thermal vaporization of volatile substances after moisture evaporation. Additionally, the complexes decomposed in two stages, with the second involving removing molecules, leading to deterioration. Similar two-stage decomposition and dehydration were also observed in the Schiff and Mannich bases. The findings suggest that the complexes and bases underwent a multi-stage decomposition process, starting with the vaporization of volatile substances followed by the deterioration and removal of molecules from the complexes during subsequent stages.

Anti-cancer Assay

The pharmaceutical investigation currently stands as the most slashing domain for identifying viable cancer treatments, with a specific focus on the creation of metal-based anticancer drugs. Since most of the medicines currently used to treat cancer are cytotoxic [19],

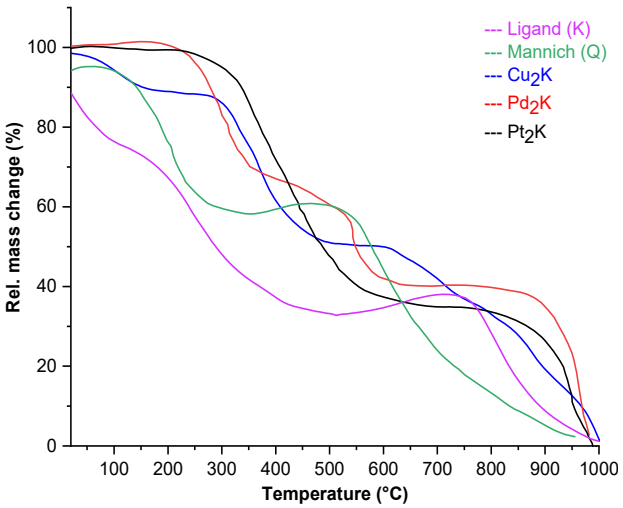

Fig 7. TG curve of the ligand and its complexes

Table 4. Data regarding the thermal decomposition of the Schiff base ligand (K), Mannich base (Q), and the corresponding complexes

Comp.	Molecular formula M.wt.	Steps	Temp. range of the decomposition (T.G) °C	The suggested formula for loss	Mass loss %	
					Cal.	Found
K	$C_{28}H_{22}N_8O_2S_2$ 566.66	1	0–200	CH_3CH_2OH, 2-OH	14.11	13.72
		2	200–390	2(-C_6H_4, -CH)	31.41	29.87
		3	390–595	2(4-N, 2-CH, 2-SH)	52.23	51.76
Q	$C_{44}H_{40}N_{10}O_2S_2$ 804.99	1	0–225	2(-OH, -C_6H_4, -CH)	26.33	25.29
		2	225–410	2(4-N, 2 -CH, 2-SH)	36.77	36.32
		3	410–595	2(-CH_2, -CH_3, C_6H_5, -N)	29.81	28.19
Cu_2K	$C_{28}H_{32}Cl_4Cu_2N_8O_6S_2$ 909.63	1	0–190	2(H_2O, -OH)	7.69	6.99
		2	190–390	2(-C_6H_4, C=C, C_2N_3H)	33.31	33.02
		3	390–595	C_6H_4	8.35	8.08
Pd_2K	$C_{28}H_{32}Cl_4N_8O_6Pd_2S_2$ 995.37	1	0–250	2 -OH, C_6H_4	11.05	10.88
		2	250–390	2 -$C_2N_3H_2$	13.66	12.83
		3	390–595	2(-C_6H_4, C=C, C=N)	25.31	23.96
Pt_2K	$C_{28}H_{24}Cl_8N_8O_2Pt_2S_2$ 1242.44	1	0–235	CH_3CH_2OH	3.70	3.54
		2	235–420	2(-OH, C=C, C_6H_4)	18.83	17.90
		3	420–595	2(-$C_2N_3H_2$)	17.06	16.72

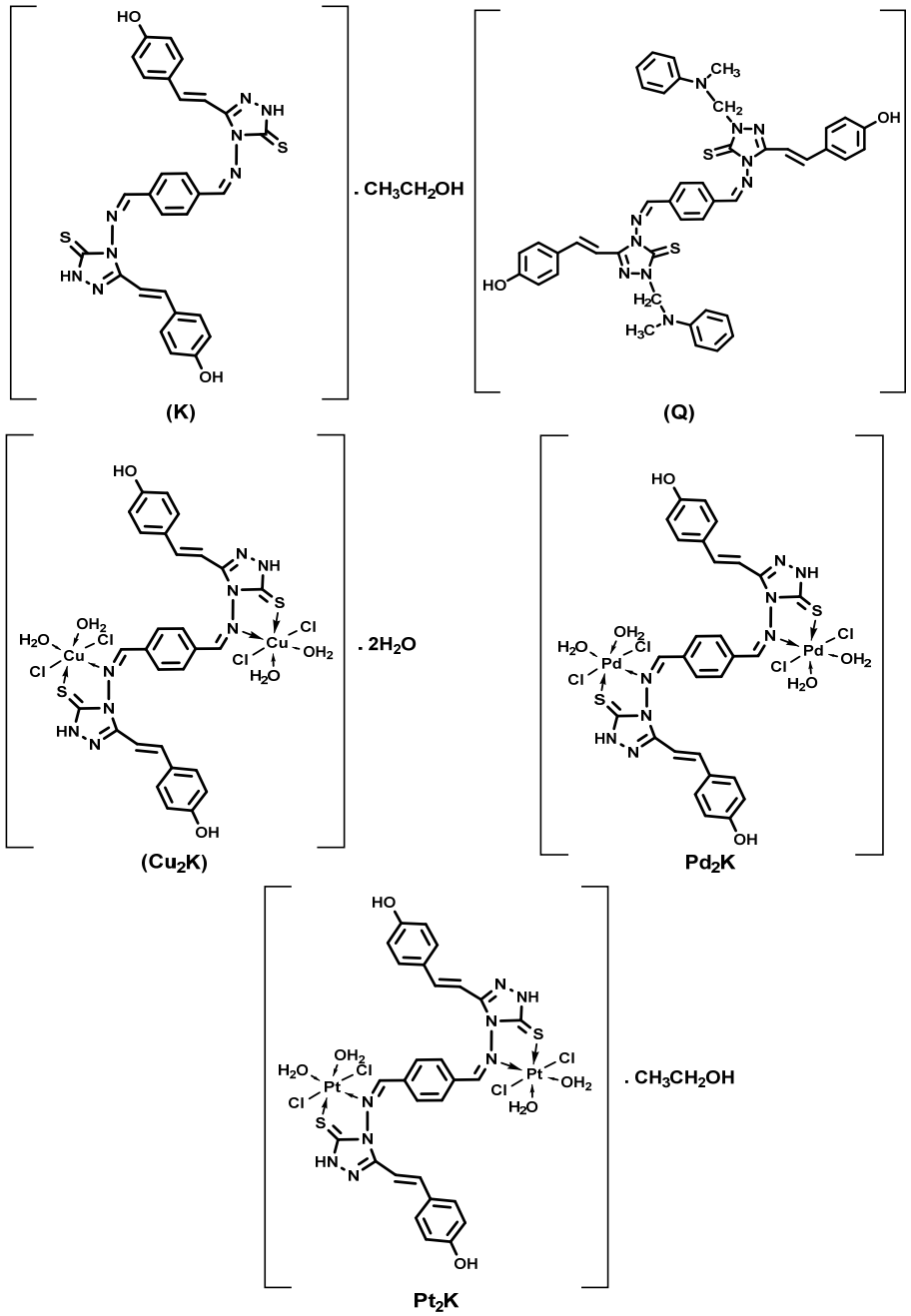

Scheme 2. The proposed structures for the Schiff base ligand (K), Mannich base (Q), and the complexes formed by these ligands with their respective metal ions

generating anticancer therapeutics with high efficacy and low toxicity is among the toughest challenges. One of the severe health burdens in the globe is the prevalence of cancer, which contributed to 1/6 (9.6 million) of the deaths worldwide in 2018. Additionally, breast cancer is the most common type of cancer diagnosed worldwide.

Chemotherapy is one of the widely used treatment programs for treating tumors, especially among women. Nevertheless, the absence of solutions and growth in drug resistance hinders the efficiency of cancer chemotherapy. Such difficulty promotes the creation of antitumor medicines that are extremely effective and have low toxicity. The heterocyclic nucleus of 1,2,4-triazole derivatives represented a much intriguing class

of substances with a broad range of biological activity. Due to their therapeutic potential, 1,2,4-triazole derivatives constitute a significant family of compounds, and many medications now contain a triazole ring. The major aims for enhancing the pharmaceutical effectiveness of triazole derivatives are their structural characteristics, such as appropriate dielectric, hydrogen bonding ability, inflexibility, and stability under *in vitro* conditions. Some drugs with a 1,2,4-triazole nucleus are utilized more medicinally, including ribavirin [20-21] (antiviral; anti-infective), itraconazole [22] (antifungal), bitertanol [23] (fungicide), and triazophos [24] (pesticide). Whereas vorozole, letrozole, and anastrozole are nonsteroidal medications used to treat cancer, while fluconazole is often utilized as an antibacterial. Aside from being used in the manufacture of numerous prospective and strong anticancer medicines, Schiff bases are particularly significant molecules with an azomethane functional group that engage in a variety of biological processes [25]. The biological activity of Schiff and Mannich bases can be enhanced when complexed with diverse transition metal ions due to their catalytic, anticancer, antibacterial, and antifungal characteristics as well as their biological production. Furthermore, organometallic Schiff bases and their transition metal complexes are regarded as significant substances. The growth of incredibly effective mineral-based drugs with applications in the treatment of infectious diseases or cancer has indeed been made possible by the complexes of *N*-heterocyclic (N–H–C) ligands with metals. The complexes were evaluated biologically, and transitional minerals demonstrated promising biological properties. This study utilized the human breast cancer cell line MCF-7 at varying concentrations (6.125, 12.5, 25, 50, and 100 g/mL) for 72 h to evaluate the synthetic compound (K, Q, Cu_2K, Pd_2K, and Pt_2K) as anti-proliferative and anti-tubulin activities by targeting tubulin protein [26]. The outcomes indicated that the new chemicals affected MCF-7 cell proliferation through such a tubulin-targeting mechanism. The findings of this investigation suggested that unique synthetic chemicals constitute new prospective therapeutic agents for the treatment of tumors.

Analytical Statistics

The data were analyzed using GraphPad Prism 5 (GraphPad Software, USA) and the statistically significant differences were evaluated by unpaired t-test with a probability level of $^*P < 0.05$. The values were exhibited as the standard error of means.

Anti-tumor Activity

The antitumor activity of various drugs was assessed in this study, specifically focusing on their cytotoxic effects on tumor cells and their ability to inhibit cell proliferation. Ligands, Schiff (K), and Mannich (Q) bases compounds, along with their complexes, were examined to determine their effectiveness against tumor cells. The study utilized the MTT assay [27] to quantify and select the appropriate concentrations of these complexes. It was observed that metal ion complexes derived from Schiff bases exhibited enhanced cytotoxicity against cancer cells, particularly those responsible for breast and brain tumors. The composition of the ligands and the functional groups used in their synthesis impacted the extent and nature of the inhibition observed.

Inhibition of Human Breast Cancer Cells (MCF-7) by the Ligand (Schiff, Mannich Bases and Other Complexes (K, Q, Cu_2K, Pd_2K, and Pt_2K)

In the MCF-7 cells, the ligand Schiff base (K) emerged in the inhibition rate of IR = 23.16% at the concentration of 100 µg/mL. The proliferation rate (PR = 4.98%) was statistically significant at the concentration of 6.25 µg/mL. As shown in Fig. 8 and Table 5, the influence of cytotoxicity was recorded at 9.12, 14.11, and 19.56% at the concentrations of 12.5, 25, and 50 µg/mL, respectively.

Breast cancer with ligand Mannich base (Q) culminated in an inhibition rate of IR = 64.13% at the concentration of C = 100 µg/mL. The proliferation rate PR = 13.22% was statistically significant at the concentration of 6.25 µg/mL. As shown in Fig. 9 and Table 5, the influence of cytotoxicity was 17.58, 23.09, and 28.22 at the concentrations of 12.5, 25, and 50 µg/mL, respectively.

Complex-(Cu_2K) emerged in the MCF-7 cells at the inhibition rate of IR = 25.26% at the concentration of 100 µg/mL. The proliferation rate PR = 6.21% was statistically significant at the concentration of 6.25 µg/mL. As shown in Fig. 10 and Table 5, the influence of cytotoxicity was recorded at 11.42, 16.21, and 22.67 at the concentrations of 12.5, 25, and 50 µg/mL, respectively.

Meanwhile, complex-(Pd_2K) emerged in the MCF-7 cells at the inhibition rate of IR = 28.09% at the concentration of 100 µg/mL. The proliferation rate PR = 8.61% was statistically significant at the concentration of 6.25 µg/mL. As shown in Fig. 11 and Table 5, the influence of cytotoxicity was recorded at 13.86, 17.58, and 24.61% at the concentrations of 12.5, 25, and 50 µg/mL.

Finally, the complex-(Pt_2K) emerged in the MCF-7 cells at the inhibition rate of IR = 68.31% at the concentration of C = 100 µg/mL. The proliferation rate PR = 14.97% was statistically significant at the concentration of C = 6.25 µg/mL. As shown in Fig. 12 and Table 5, the influence of cytotoxicity was recorded at 19.36, 24.93, and 31.60 at concentrations of 12.5, 25, and 50 µg/mL.

Table 5. Cytotoxicity assays of MCF-7 cells for K, Q, Cu_2K, Pd_2K, and Pt_2K

Comp.	IR%, (C) µg/mL	PR%, (C) µg/mL	Other effect cytotoxicity%, (C) µg/mL		
K	23.16 (100)	4.98 (6.25)	9.12 (12.5)	14.11 (25)	19.56 (50)
Q	64.13 (100)	13.22 (6.25)	17.58 (12.5)	23.09 (25)	28.22 (50)
Cu_2K	25.26 (100)	6.21 (6.25)	11.42 (12.5)	16.21 (25)	22.67 (50)
Pd_2K	28.09 (100)	8.61 (6.25)	13.86 (12.5)	17.58 (25)	24.61 (50)
Pt_2K	68.31 (100)	14.97 (6.25)	19.36 (12.5)	24.93 (25)	31.60 (50)

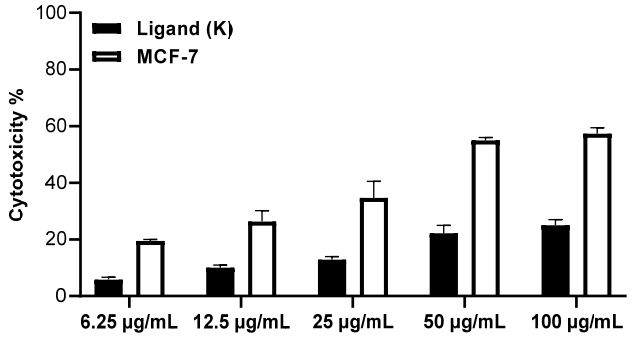

Fig 8. Cytotoxicity of Schiff base (K) against MCF-7 cells

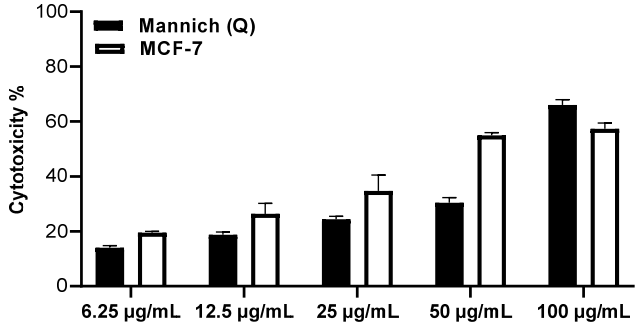

Fig 9. Cytotoxicity of Mannich base (Q) against MCF-7 cells

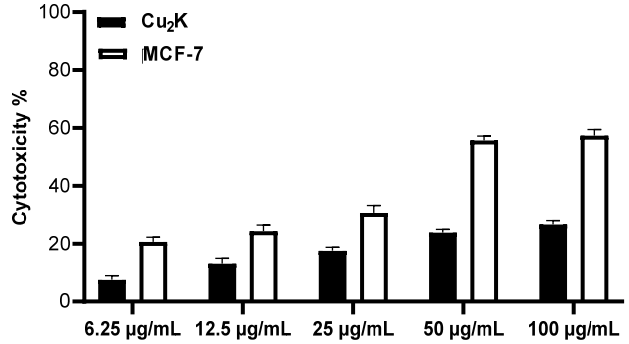

Fig 10. Cytotoxicity of Cu_2K against MCF-7 cells

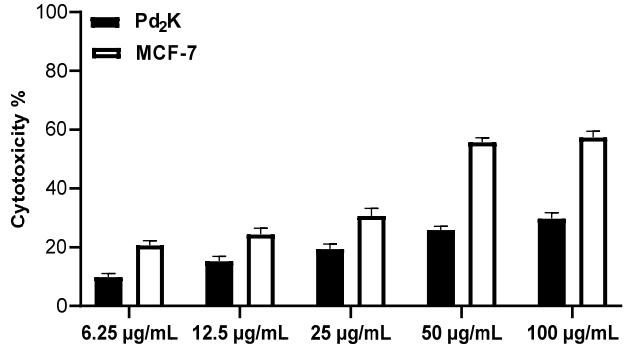

Fig 11. Cytotoxicity of Pd_2K against MCF-7 cells

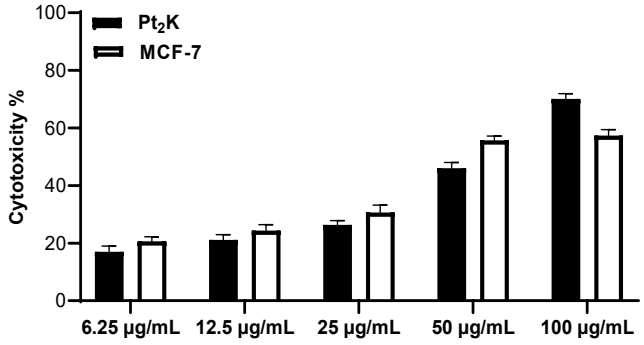

Fig 12. Cytotoxicity of Pt_2K against MCF-7 cells

The Evaluation of Compounds to Initiate Apoptosis

Although chromatin condensation levels differ in apoptotic cells [28], they often display red to pink-colored nuclei. Fig. 13 shows the use of AO/EtBr dye combinations to further explore the tested compounds' ability to cause cancer cell line death [29]. The cell nuclei's morphology and dark red color remained stable; however, when cancer cells were treated with a new experimental compound, their membranes were less consistent than those of untreated cells [30]. The morphological changes in the treated MCF-7 cells indicated that apoptosis was the primary reason for the observed cell death. At low doses, these compounds showed potent anti-proliferative effects against the MCF-7 cells. The presence of an azo-methane group CH=N in the Schiff base's (K) chelate ring and a methylene group in the Mannich base (Q) may contribute to the enhanced activities of the synthesized compounds, as this element reduced the metal atoms' polarity during the coordination of metal ions with nitrogen. Besides the role of the employed complexes, the platinum and palladium complexes, along with the copper complex, were also observed to exhibit apoptosis effects against the MCF-7 cells.

■ CONCLUSION

The Schiff base ligand (K) was synthesized using a derivative of the triazole ring with terephthaldehyde, following a procedure outlined in the literature. Additionally, the Mannich base ligand (Q) was synthesized by reacting Schiff base (K) with *N*-methyl aniline and methylene oxide using a procedure reported in the literature. The newly synthesized ligands (K) exhibited a bi-dentate behavior in their metal complexes, specifically copper(II), palladium(II), and platinum(IV) metal ions. These metal ions coordinated with the thiol group and nitrogen of dimethyldiazene. The MTT experiment, which utilized the MCF-7 cell line, yielded interesting findings. The results indicated that certain synthetic compounds, even at low concentrations, have the potential to inhibit the proliferation of cancer cells. This suggests their potential as inhibitors for breast cancer MCF-7. The platinum complex exhibited the highest rate of inhibition and apoptosis of breast cancer cells MCF-7, with an inhibition rate (IR) of 64.13% and a concentration of 100 µg/mL. Conversely, the lowest rate

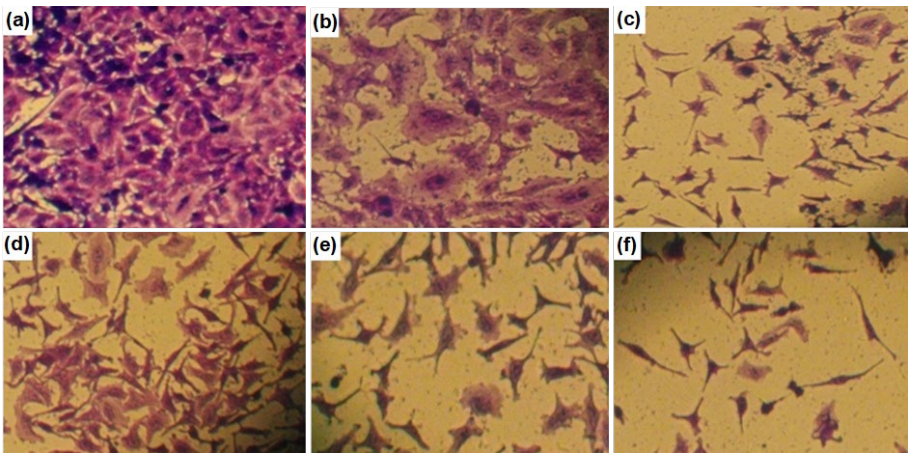

Fig 13. Representative photomicrographs of the cellular morphology of (a) untreated MCF-7 cells, (b) ligand K Schiff base, (c) ligand Q Mannich base, (d) Cu_2K complex, (e) Pd_2K complex, and (f) Pt_2K complex. Images were taken at 40× magnification by using a microscope TE-2000 (Nikon, Japan), scale bar: 50 µM

of inhibition and apoptosis was observed in untreated cells. Based on the outcomes, the order of effectiveness was determined to be: Pt_2K > Q > Pd_2K > Cu_2K > K > untreated cells. Through *in vitro* results, we conclude that the prepared compounds have a promising future in apoptosis and inhibition of breast cancer cells.

■ ACKNOWLEDGMENTS

We wish to express our gratitude to both the Baghdad and Mustansiriyah Universities, Iraq, the faculty of Science, Osmania University, India for their technical assistance.

■ REFERENCES

[1] Wei, L., Chang, X., and Wang, C.J., 2020, Catalytic asymmetric reactions with *N*-metallated azomethine ylides, *Acc. Chem. Res.*, 53 (5), 1084–1100.

[2] Raczuk, E., Dmochowska, B., Samaszko-Fiertek, J., and Madaj, J., 2022, Different Schiff bases–Structure, importance and classification, *Molecules*, 27 (3), 787.

[3] Al-Khazraji, A.M., and Al Hassani, R.A., 2020, Synthesis, characterization and spectroscopic study of new metal complexes form heterocyclic compounds for photostability study, *Sys. Rev. Pharm.*, 11 (5), 535–555.

[4] Abd Razak, N., Abu, N., Ho, W.Y., Zamberi, N.R., Tan, S.W., Alitheen, N.B., Long, K., and Yeap, S.K., 2019, Cytotoxicity of eupatorin in MCF-7 and MDA-MB-231 human breast cancer cells via cell cycle arrest, anti-angiogenesis and induction of apoptosis, *Sci. Rep.*, 9 (1), 1514.

[5] Lindhagen, E., Nygren, P., and Larsson, R., 2008, The fluorometric microculture cytotoxicity assay, *Nat. Protoc.*, 3 (8), 1364–1369.

[6] Al-Khazraji, A.M.A., 2023, Synthesis of Co(II), Ni(II), Cu(II), Pd(II), and Pt(IV) complexes with 1^4,1^5,3^4,3^5-tetrahydro-1^1H,3^1H-4,8-diaza-1,3(3,4)-ditriazola-2,6(1,4)-dibenzenacyclooctaphane-4,7-dien-1^5,3^5-dithione, and the thermal stability of polyvinyl chloride modified complexes, *Indones. J. Chem.*, 23 (3), 754–769.

[7] Al-Ezzy, R.M., Alshanon, A.F., and Khalaf, H.M., 2023, Studying some cytotoxic and cytogenetic potentials of Dandelion methanolic extract on MCF-7 cancer cell line: An *in vitro* study, *Iraqi J. Sci.*, 64 (3), 1160–1170.

[8] Baldwin, E.L., and Osheroff, N., 2005, Etoposide, topoisomerase II and cancer, *Curr. Med. Chem.: Anti-Cancer Agents*, 5 (4), 363–372.

[9] Fusco, R., Cordaro, M., Siracusa, R., Peritore, A.F., D'Amico, R., Licata, P., Crupi, R., and Gugliandolo, E., 2020, Effects of hydroxytyrosol against lipopolysaccharide-induced inflammation and oxidative stress in bovine mammary epithelial cells: A natural therapeutic tool for bovine mastitis, *Antioxidants*, 9 (8), 693.

[10] Wang, H., and Mao, X., 2020, Evaluation of the efficacy of neoadjuvant chemotherapy for breast cancer, *Drug Des., Dev. Ther.*, 14, 2423–2433.

[11] Aswathanarayanappa, C., Bheemappa, E., Bodke, Y.D., Krishnegowda, P.S., Venkata, S.P., and Ningegowda, R., 2013, Synthesis and evaluation of antioxidant properties of novel 1,2,4-triazole-based Schiff base heterocycles, *Arch. Pharm.*, 346 (12), 922–930.

[12] Seelam, N., Shrivastava, S., Prasanthi, S., and Gupta, S., 2016, Synthesis and *in vitro* study of some fused 1,2,4-triazole derivatives as antimycobacterial agents, *J. Saudi Chem. Soc.*, 20 (4), 411–418.

[13] Lehrich, B.M., Liang, Y., and Fiandaca, M.S., 2021, Foetal bovine serum influence on *in vitro* extracellular vesicle analyses, *J. Extracell. Vesicles*, 10 (3), e12061.

[14] Tamer, T.M., Sabet, M.M., Omer, A.M., Abbas, E., Eid, A.I., Mohy-Eldin, M.S., and Hassan, M.A., 2021, Hemostatic and antibacterial PVA/Kaolin composite sponges loaded with penicillin–streptomycin for wound dressing applications, *Sci. Rep.*, 11 (1), 3428.

[15] Vajta, G., and Kuwayama, M., 2006, Improving cryopreservation systems, *Theriogenology*, 65 (1), 236–244.

[16] Al-Khazraji, A.M., Al Hassani, R.A., and Ahmed, A., 2020, Studies on the photostability of polystyrene films with new metals complex of 1,2,4-triazole-3-thione derivate, *Sys. Rev. Pharm.*, 11 (5), 525–534.

[17] Hozien, Z.A., El-Mahdy, A.F., Abo Markeb, A., Ali, L.S.A., and El-Sherief, H.A.H., 2020, Synthesis of Schiff and Mannich bases of new *s*-triazole derivatives and their potential applications for removal of heavy metals from aqueous solution and as antimicrobial agents, *RSC Adv.*, 10 (34), 20184–20194.

[18] Hossain, N., Zaini, J., Mahlia, T., and Azad, A.K., 2019, Elemental, morphological and thermal analysis of mixed microalgae species from drain water, *Renewable Energy*, 131, 617–624.

[19] Pérez, S., Montalbán, M.G., Carissimi, G., Licence, P., and Víllora, G., 2020, *In vitro* cytotoxicity assessment of monocationic and dicationic pyridinium-based ionic liquids on HeLa, MCF-7, BGM and EA.hy926 cell lines, *J. Hazard. Mater.*, 385, 121513.

[20] Casaos, J., Gorelick, N.L., Huq, S., Choi, J., Xia, Y., Serra, R., Felder, R., Lott, T., Kast, R.E., Suk, I., Brem, H., Tyler, B., and Skuli, N., 2019, The use of ribavirin as an anticancer therapeutic: Will it go viral?, *Mol. Cancer Ther.*, 18 (7), 1185–1194.

[21] Ianevski, A., Yao, R., Biza, S., Zusinaite, E., Mannik, A., Kivi, G., Planken, A., Kurg, K., Tombak, E.M., Ustav, Jr. M., Shtaida, N., Kulesskiy, E., Jo, E., Yang, J., Lysvand, H., Løseth, K., Oksenych, V., Aas, P.A., Tenson, T., Vitkauskienė, A., Windisch, M.P., Fenstad, M.H., Nordbø, S.A., Ustav, M., Bjørås, M., and Kainov, D.E., 2020, Identification and tracking of antiviral drug combinations, *Viruses*, 12 (10), 1178.

[22] El-Sheridy, N.A., El-Moslemany, R.M., Ramadan, A.A., Helmy, M.W., and El-Khordagui, L.K., 2021, Enhancing the *in vitro* and *in vivo* activity of itraconazole against breast cancer using miltefosine-modified lipid nanocapsules, *Drug Delivery*, 28 (1), 906–919.

[23] Li, L., Gao, B., Wen, Y., Zhang, Z., Chen, R., He, Z., Kaziem, A.E., Shi, H., and Wang, M., 2020, Stereoselective bioactivity, toxicity and degradation of the chiral triazole fungicide bitertanol, *Pest. Manage. Sci.*, 76 (1), 343–349.

[24] Yang, F.W., Li, Y.X., Ren, F.Z., Wang, R., and Pang, G.F., 2019, Toxicity, residue, degradation and detection methods of the insecticide triazophos, *Environ. Chem. Lett.*, 17 (4), 1769–1785.

[25] Deepthi, A., Thomas, N.V., and Sruthi, S.L., 2021, An overview of the reactions involving azomethine imines over half a decade, *New J. Chem.*, 45 (20), 8847–8873.

[26] Barreca, M., Stathis, A., Barraja, P., Bertoni, F., 2020, An overview on anti-tubulin agents for the treatment of lymphoma patients, *Pharmacol. Ther.*, 211, 107552.

[27] Ciapetti, G., Cenni, E., Pratelli, L., and Pizzoferrato, A., 1993, *In vitro* evaluation of cell/biomaterial interaction by MTT assay, *Biomaterials*, 14 (5), 359–364.

[28] Xu, X., Lai, Y., and Hua, Z.C., 2019, Apoptosis and apoptotic body: Disease message and therapeutic target potentials, *Biosci. Rep.*, 39 (1), BSR20180992.

[29] Olmsted III, J., and Kearns, D.R., 1977, Mechanism of ethidium bromide fluorescence enhancement on binding to nucleic acids, *Biochemistry*, 16 (16), 3647–3654.

[30] Fischer, E.G., 2020, Nuclear morphology and the biology of cancer cells, *Acta Cytol.*, 64 (6), 511–519.